

# An integrated transceiver based on a reflective semiconductor optical amplifier for the access network

L. Xu, X.J.M. Leijtens, J.H. den Besten, M.J.H. Sander-Jochem,  
T. de Vries, Y.S. Oei, P.J. van Veldhoven, R. Nötzel and M.K. Smit

COBRA Research Institute, Technische Universiteit Eindhoven  
Postbus 513, 5600 MB Eindhoven, The Netherlands

*In this paper, a reflective transceiver is presented which monolithically integrates a wavelength duplexer, a reflective SOA (RSOA) and a detector. The first characterization shows that the wavelength duplexer obtained better than  $-15$  dB optical isolation between the upstream and downstream signals. The polarization dependence was less than 25% of the 200 GHz (1.6 nm) channel spacing over a 50 nm wavelength range. A 750  $\mu\text{m}$  long RSOA achieved around 20 dB on-chip gain, and a 30  $\mu\text{m}$  long photodetector shows good responsivity of up to 0.25-0.4 A/W within a 50 nm operating range at  $-2$  V bias voltage.*

## Introduction

With the dramatic increase in the number of the subscribers and their demands on the speed and bandwidth capacities, the substitution at the user side of the usual media such as coaxial cable with the optical fiber is inevitable. A transceiver at the user side performs the tasks to transform the data in the download stream carried by the light inside the fiber into electrical information, and to upload the electrical data stream from the user side into the optical information suitable for the fiber transmission. The performance and cost of the transceiver will directly influence the whole system deployment. Previous research has demonstrated up to 1.25 Gbit/s transceiver (ONU) for the download and upload streams by using discrete components: a wavelength duplexer, a laser[1] or a RSOA[2] as transmitter, and a photodetector.

However, due to the cost, it is not practical to deploy such a transceiver with discrete components at the user side. In this paper, we present a reflective transceiver which monolithically integrates the above discrete components within one chip, fig. 1. This device is designed for the Dutch Broadband Photonics project, in which the wavelengths are dynamically allocated. The wavelengths which will carry the data are assigned by the local exchange, according to the network requirements. Therefore the transceiver has to be wavelength agnostic. We chose to use a RSOA as a transmitter, because in that way the wavelength is specified by the local exchange and modulated and reflected at the user side.

The module works with two wavelengths ( $\lambda_1$  and  $\lambda_2$ ) spaced 200 GHz coming from the network into the transceiver, where they will be separated by the wavelength duplexer and guided to the photodetector ( $\lambda_1$ ) and the RSOA modulator ( $\lambda_2$ ). The downstream data, carried by  $\lambda_1$ , is detected by the photodetector, while  $\lambda_2$  is a continuous wave (CW) light

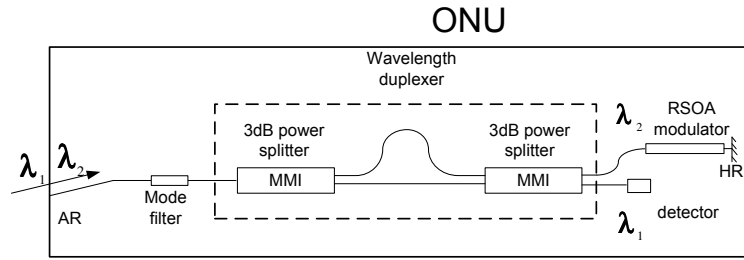


Figure 1: Integrated transceiver consisting of a wavelength duplexer, a reflective SOA modulator and a detector.

and is guided to the RSOA where it is modulated, amplified and reflected back to the network. The RSOA is realized by applying a high reflectivity coating (HR) at the one side of the chip. To avoid lasing, the other facet of the chip, where the light is coupled into and out of the device, is provided with an anti-reflection coating (AR). An angled input waveguide and a mode filter are used to further minimize the reflections from that facet. The wavelength duplexer is designed to be polarization insensitive by proper waveguide geometry design. The detailed modeling and simulation of the layers, waveguides, mode filter, and MMI can be found in [3]. The modulation of the upstream data is carried out by changing the driving current of the RSOA. The photodetector and the RSOA in this device share the same PIN layer structure, but work under the different bias conditions.

## Fabrication and characterization of the transceiver

The material we used is grown on an N-type InP substrate by a three-step low pressure metal-organic-vapor-phase epitaxy (MOVPE) at 625 °C. The SOA active layer consists of 120 nm thick Q1.55 ( $\lambda_{\text{gap}} = 1.55 \mu\text{m}$ ) InGaAsP layer embedded between two quaternary confinement layers. The structure was covered by a 200 nm thick p-InP layer. Next, the active sections were defined by lithography and reactive ion etching (RIE) using a  $\text{SiN}_x$  layer as etching mask. In the second epitaxy step, a Q1.25 InGaAsP layer was selectively grown for the passive sections with the  $\text{SiN}_x$  mask protecting the active sections[4]. In the third epitaxy step, a 1300 nm thick p-InP cladding layer and p-InGaAs contacting layer were grown.

In the transceiver, all access waveguides, photodetector and RSOA are shallowly etched, 100 nm into the Q1.25 film layer by RIE, to minimize the transmission loss and the surface recombination. The multimode interference couplers (MMIs) and the 1.5  $\mu\text{m}$ -wide Mach-Zehnder arms are etched completely through the waveguiding layer, giving stronger lateral confinement to allow for smaller radii and better fabrication tolerance for the MMIs. Polyimide was spun for passivation and planarization. By etching back the polyimide, the Ti/Pt/Au metal can be evaporated on the p-InGaAs contact layer to form the electrodes on the top and the ground (n-InP) at the backside. After annealing and cleaving, the chip was soldered on a copper chuck with a Peltier cooler for the characterization.

The first measurement was done on the duplexer, and the results are shown in fig. 2. The vertical axis shows the transmission of the duplexer, normalized to a deeply etched straight waveguide. The isolation between two datastreams is better than 15 dB. The measured channel spacing between the downstream and upstream wavelength is about 205 GHz.

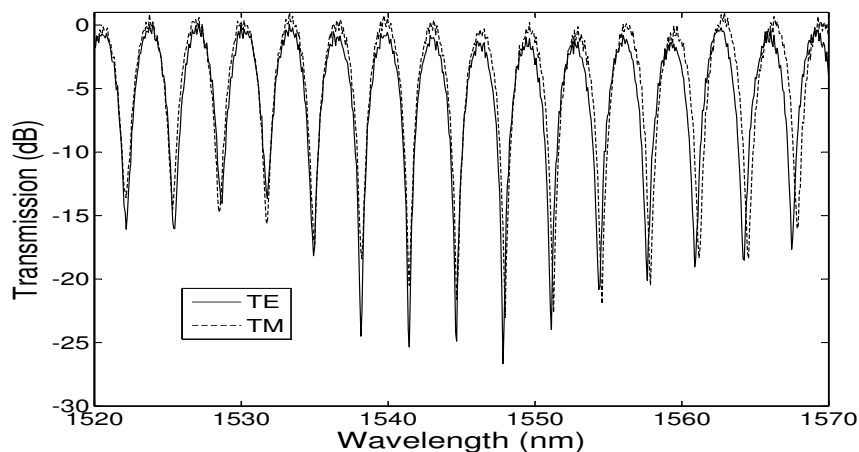


Figure 2: A polarization independent wavelength duplexer

The peak transmission shift between TE and TM polarized light is less than 25% of the 200 GHz (1.6 nm) channel spacing, within the range of 1520 nm to 1570 nm.

To obtain high gain and high signal extinction ratio, the RSOA preferably works at high injection current, but below the lasing threshold. The size of the measured RSOA is  $750\ \mu\text{m}$  long and  $2\ \mu\text{m}$  wide. The HR facet has 99% reflectivity, and the AR facet at the input side has 0.1% reflectivity. With these values, the lasing threshold of the RSOA was predicted to be around 150 mA through rate-equation-based modeling, while the measured value was about 100 mA. The cause of this discrepancy is the residual reflections. The influence of these residual reflections, together with a heating effect, was also observed on the gain curve which bends at higher injection current near to lasing threshold, as is shown in fig. 3. Several reflection cavities between active-passive butt-joints and facets are observed by analyzing a high resolution optical spectrum with a Fourier transformation[5]. In a next design, residual reflections will be further suppressed by angling the waveguides entering the active material[4], and using adiabatic curves to avoid possible reflections at waveguide junctions.

The modulation speed of the RSOA is limited mostly by the spontaneous carrier lifetime which is shortened with higher injection current. For an InP based SOA the carrier lifetime is on the order of hundreds of picoseconds, thus corresponding to GHz modulation rates.

The photodetector has the same layer structure as the RSOA, but works under reverse bias. We fabricated detectors with lengths ranging from  $30\ \mu\text{m}$  to  $60\ \mu\text{m}$ . Here we present the measurements of the  $30\ \mu\text{m}$ -long and  $2\ \mu\text{m}$ -wide detector. The dark current of the photodetector is less than 50 nA at  $-5\ \text{V}$  reverse bias voltage. The measured responsivity, shown in fig. 4, is up to  $0.25\sim 0.4\ \text{A/W}$  (corresponding to 60%~90% internal quantum efficiency if the fiber chip coupling loss is estimated at  $-4.3\ \text{dB}$ ) in operating range at  $-2\ \text{V}$  bias. The estimated bandwidth for this detector is up to 25 GHz based on RC and carrier transit time calculation.

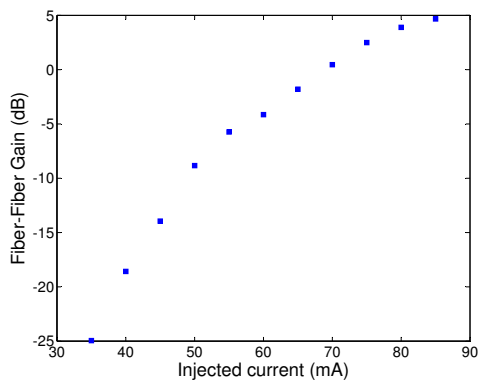


Figure 3: Measured device gain increased with the injection current for  $\lambda_{\text{peak}} = 1523.6\text{nm}$ , and  $P_{\text{optin}} = -15\text{dBm}$ .

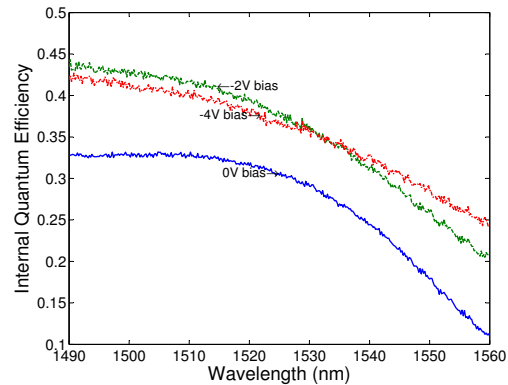


Figure 4: Responsivity of a  $30\mu\text{m}$  long detector as a function of the wavelength at different reverse-bias voltages.

## Conclusion

In this paper, we realized a first integrated transceiver with a wavelength duplexer, a RSOA modulator and a photodetector. It gives better than 15 dB isolation between downstream and upstream data, and a polarization dependence smaller than 25% of the 200 GHz (1.6 nm) channel spacing within 50 nm wavelength range, over 5 dB fiber-fiber gain at 85 mA injection current, and a good responsivity for a  $30\mu\text{m}$ -long photodetector, 0.25~0.4 A/W at  $-2\text{V}$  reverse bias.

This work is partly funded by the Dutch National Broadband Photonics Access project.

## References

- [1] J. Endo, M. Nakamura, Y. Umeda, and Y. Akatsu, "1.25 Gbit/s optical transceiver with high sensitivity and high speed response for GE-PON systems," in *2005 Conference on Lasers and Electro-Optics (CLEO)*, 2005, pp. 1496–1497.
- [2] J. Prat, C. Arellano, V. Polo, and C. Bock, "Optical network unit based on a bidirectional reflective semiconductor optical amplifier for fiber-to-the-home networks," *IEEE Photon. Technol. Lett.*, vol. 17, no. 1, pp. 250–252, Jan. 2005.
- [3] L. Xu, X. Leijtens, M. Sander-Jochem, Y. Oei, and M. Smit, "Modeling and design of a high-speed reflective transceiver for the access network," in *Proc. IEEE/LEOS Symposium (Benelux Chapter)*. Mons, Belgium, Dec. 2005, pp. 137–140.
- [4] Y. Barbarin, E. Bente, C. Marquet, E. Leclère, T. de Vries, P. van Veldhoven, Y. Oei, R. Nötzel, M. Smit, and J. Binsma, "Butt-joint reflectivity and loss in InGaAsP/InP waveguides," in *Proc. 12th Eur. Conf. on Int. Opt. (ECIO '05)*. Grenoble, France, April 6–8 2005, pp. 406–409.
- [5] D. Ackerman, L. Zhang, L.-P. Ketelsen, and J. Johnson, "Characterizing residual reflections within semiconductor lasers, integrated sources, and coupling optics," *IEEE J. Quantum Electron.*, vol. 34, no. 7, pp. 1224–1230, July 1998.